Selective magnetic resonance imaging of magnetic nanoparticles by Acoustically Induced Rotary Saturation (AIRS)

Bo Zhu[1,2], Thomas Witzel[1], Shan Jiang[3], Susie Y. Huang[1], Bruce R. Rosen[1,4], and Lawrence L. Wald[1,2]

[1]*Martinos Center for Biomedical Imaging, Department of Radiology, Massachusetts General Hospital, Charlestown, MA, United States,* [2]*Harvard-MIT Division of Health Sciences Technology, Massachusetts Institute of Technology, Cambridge, MA, United States,* [3]*David H Koch Institute for Integrative Cancer Research, Department of Chemical Engineering, Massachusetts Institute of Technology, Cambridge, MA, United States,* [4]*Department of Meridian & Acupuncture, Collaborating Center for Traditional Medicine, East-West Medi, Kyung Hee University, Seoul, Korea*

Introduction: The presence of magnetic nanoparticle contrast agents is typically manually determined by locating hypointense regions from conventional T_2- or T_2^*-weighted acquisitions, which is problematic in complex tissue backgrounds with other naturally occurring regions of dark contrast, particularly for low agent concentrations. Pre- and post-injection comparisons which seek to account for this limitation are susceptible to other confounding sources of contrast change introduced by the often lengthy inter-scan duration necessitated by the generally slow biodistribution times of these agents; subject motion, internal organ movement, scanner drift, and other irrelevant modulations in signal intensity make subtractive imaging and other quantitative pre-/postcomparison methods infeasible. Here we present an entirely post-injection method which achieves rapid and repeatable contrast modulation (as opposed to slow and one-time via pre-/post- injection) by establishing a rotating frame resonance condition between the spin-locked water magnetization and the oscillating magnetic fields generated by mechanically or acoustically vibrated contrast agents. In the Rotary Saturation effect [1], the spin-locked magnetization undergoes a nutation by an externally applied audio-frequency oscillating field tuned to $\omega_{spin\_lock}=\gamma B_{1spin\_lock}$ which results in a signal intensity change (Fig. 1a) after flipback to the longitudinal axis and image readout (Fig. 1b). Because a vibrating magnetic particle or accumulation of particles can generate this field, this Acoustically Induced Rotary Saturation (AIRS) method can be used to "activate" the contrast effect by applying the resonant vibration frequency [2-4]. Because only spins near the oscillating fields of the nanoparticles experience this nutated magnetization, we can selectively detect the location of these agents by performing a statistical analysis of activated/on-resonance and non-activated/off-resonance conditions (Fig. 1d, 2a).

Methods: Glass spherical cell microcells containing 1) varying concentrations of 10 nm diameter Fe_2O_3 nanoparticles and 2) Fomblin® perfluoropolyether (PFPE) oil, a control fluid with low signal are both attached at one end to a piezoelectric bender actuator and the other end lowered into a liquid water phantom. A third microcell filled with the identical iron oxide concentration was also lowered into the phantom to provide a stationary control to demonstrate the effect's dependence on properly tuned vibrational motion. Driven with an audio frequency function generator and voltage amplifier, the piezo induces oscillating displacements of the samples at a chosen frequency $\omega_{rotarysat}$. A spin-lock prepared single-shot HASTE pulse sequence (Fig. 1b) is used in a Siemens Avanto 1.5T scanner to capture $T_{1\rho}$ –weighted images with 256x256 matrix, 12-cm FOV, 5mm slice thickness, TE of 67 ms, and TR of 3.0 s. Average image intensity values in the ROI of the contrast agent location are obtained in both on-resonance ($\omega_{stim}=\gamma B_{1lock}$) and off-resonance ($\omega_{rotarysat}=\gamma B_{1spin\_lock}-\Delta\omega$) conditions, where $\Delta\omega$ was 25Hz. The signal change $\Delta S/S$, was computed from the on-resonance to off-resonance signal difference, is observed while vibrational displacement of the sample varied between 10 and 500 um, Fe concentration varied from zero to 200 ug/ml, and spin-lock resonant frequency γB_{1spin_lock} was swept from 25 to 225 Hz over sample vibrations frequencies 50, 100, 150, and 200 Hz. A block design experiment was conducted by acquiring a set of 100 single-shot HASTE images while switching aforementioned resonance states in 20 image blocks. Voxel-by-voxel analysis of the signal changes between blocks was performed using standard fMRI methods (FEAT [FMRI Expert Analysis Tool] in FSL and time series statistical analysis was performed using FILM (FMRIB Improved Linear Model), and contrasts were cluster corrected at a threshold of $Z>2.3$ ($P<0.05$).

Results: The AIRS method is able to discriminate between the previously undifferentiated iron oxide and PFPE control samples (Fig. 1c) with statistical analysis of the on-/off- resonance block design experiment (Fig. 1d), whose signal modulations are particularly evident in the time courses of Fig. 2a. Moreover, the strength of the effect is quantifiable and nearly linearly dependent upon both vibrational displacement (Fig. 2c) and Fe concentrations (Fig. 2d) of the sample, as expected due to the corresponding strengths of the oscillating fields. The resonant feature of the AIRS technique is demonstrated by the frequency sweeps in Fig 2b, and closely corresponds with Bloch simulation predictions [4].

Discussion: Our experiments demonstrate the feasibility of selectively imaging iron oxide contrast agents through a contrast modulation mechanism based on the rotary saturation effect. Separation of the agent's contrast from the background may enable quicker and more accurate visualization of injected MR iron oxide contrast agents in both research and clinical settings. The characterization experiments show that the AIRS effect appears well-behaved across a number of physical parameters; of particular importance is its nearly linear correlation between effect intensity and iron oxide concentration in clinically relevant ranges, enabling not only simple visual evaluations of relative concentration levels, but also potentially the development of quantification techniques measuring contrast agent concentration. Our results indicate the AIRS contrast mechanism can be readily extended to tissue-mimicking gel phantoms and *in-vivo* settings by the application of shear waves propagating through the sample media, as the typical range of displacement amplitudes (tens of microns) already generated clinically in shear waves through tissue during MR elastography [5] has been shown effective in modulating contrast through the AIRS technique.

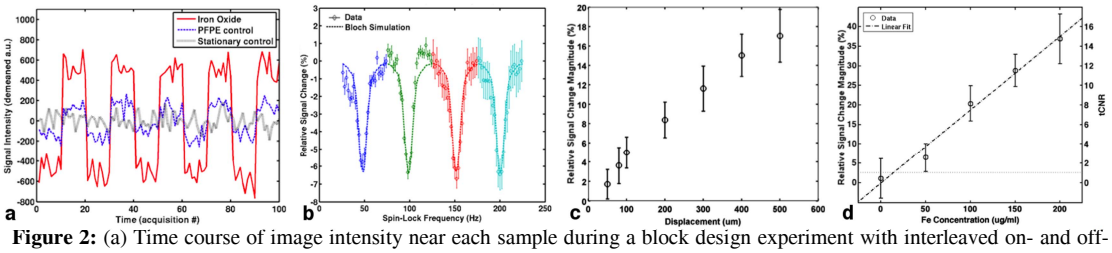

Figure 2: (a) Time course of image intensity near each sample during a block design experiment with interleaved on- and off-resonance acquisition blocks. (b) Frequency sweep of spin-lock frequency demonstrating the resonant property of the rotary saturation effect for various vibration frequencies $\omega_{rotarysat}$. (c) Magnitude of the relative signal change between on- and off-resonance conditions as a function of vibrational displacement. (d) Characterization of the AIRS effect as a function of Fe concentration alongside a linear fit with $R^2 = 0.93$.

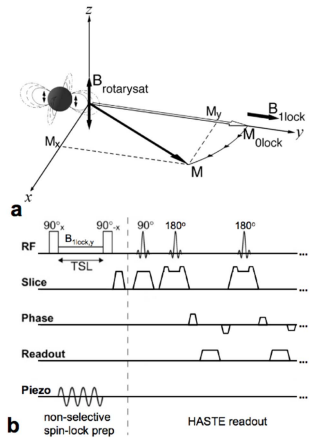

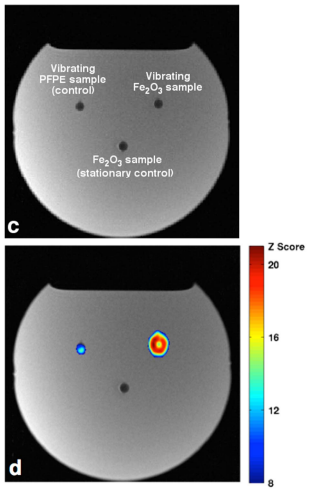

Figure 1: (a) Spin-locked magnetization near iron oxide nanoparticles vibrating at the spin-lock resonant frequency γB_{1lock} coherently rotates, modulating imaging contrast. (b) Pulse sequence diagram of spin-lock prep and subsequent HASTE readout. (c) T_2-weighted acquisition showing contrast agent and two control samples as undifferentiated hypointense regions. (d) Modulation response map of the block design experiment highlighting the vibrating contrast agent sample, generated by voxel-wise statistical analysis of intensity changes between on- and off-resonance acquisitions.

References: **1.** Redfield, A.G., 1955. *Nuclear magnetic resonance saturation and rotary saturation in solids.* Phys. Rev. 98, 1787. **2.** Zhu, B. et al., 2011. Proc. 19th ISMRM p. 123. **3.** Zhu, B. et al., 2012. Proc. 20th ISMRM p. 382. **4.** Zhu, B. et al., 2014. *Selective Magnetic Resonance Imaging of Magnetic Nanoparticles by Acoustically Induced Rotary Saturation*. Magnetic Resonance in Medicine doi: 10.1002/mrm.25522. **5.** McCracken, et al., 2004, *Transient MR Elastography: Modeling Traumatic Brain Injury,* MICCAI, LNCS 3217, pp. 1081-1082. **Acknowledgements:** This work was financially supported by P41RR14075.